DANISH METEOROLOGICAL INSTITUTE

TECHNICAL REPORT

No. 01-04

Detailed Wind Speed Information From RADARSAT ScanSAR Wide

February 2001

Rasmus Tage Tonboe

ISSN 0906-897X

Copenhagen 2001

Preface

This report is presenting the status of the work done at DMI extracting wind speeds from Radarsat SAR data in Southern Greenland. DMI is operationally receiving Radarsat ScanSAR data covering the Cape Farewell area. These data are used for ice mapping but they also contain information of the wind speed over the ocean which is an important parameter for the ice drift. This work has been done in co-operation with the German research institution GKSS in particular Jochen Horstmann. The co-operation began in 1998 and has in addition to the results presented here also resulted in a common ENVISAT data investigator project and numerous publications at international conferences and in reviewed journals.

List of contents

1. Conventions

1.1 List of symbols and abbreviations

a : Constant shaping the polarisation transfer function (Kirchoff=1)
C-band: 5.3GHz
CDPF: Canadian Data Processing Facility
CEOS: Committee on Earth Observation Satellites
CIS: Canadian Ice Service
CMOD4: C-band model version 4, for estimation of wind speed over the ocean from microwave scattering
DMI: Danish Meteorological Institute
DMSP: Defence Meteorological Satellite Program
DMSP-SSM/I: Passive microwave sensor, Special Sensor Microwave/Imager (DMSP)
DN: Digital Number
E: Spectral energy density
ENVISAT: Environmental Satellite, ESA, launch date 2000.
ERS: European Remote Sensing satellite, ESA
GKSS: GKSS Research Centre, Germany
HH: Horizontal linear polarisation
HIRLAM: High Resolution Limited Area Model
I: Incidence angle
ICE LUT: Look Up Table enhancing sea ICE features
IMSI: Integrated use of new microwave satellite data for improved sea ice observation
k: Vector wave number
MBL: Marine Boundary Layer
NOAA: National Oceanographic and Atmospheric Administration
NOAA-AVHRR: Advanced Very High Resolution Radiometer (NOAA)
NRCS: Normalised Radar Cross Section
OSIMS: Operational Sea Ice Monitoring by Satellites In Europe
Radar brightness: Radar cross Section (not compensated for incidence angle or orography)
RCS: Radar Cross Section
SAR: Synthetic Aperture Radar
ScanSAR wide: Special mode on Radarsat
T: Transfer function
VV: Vertical Linear polarisation

2. Introduction

The Greenland Ice Service at the Danish Meteorological Institute(DMI) is using satellites data for the generation of sea ice information products. The most useful data type for the ice mapping is Radarsat ScanSAR wide, but also NOAA-AVHRR and DMSP-SSM/I data are used. Effort has been invested in both developing a powerful image processing system and developing methods to enhance ice features in SAR images and in other ways aid the image interpretation and ice mapping process (Gill and Valeur, 1999). The work presented here has resulted in both the possibility for calibrating the Radarsat images and for deriving the wind speed over the sea surface using the SAR data.

Radarsat was launched and sent in orbit 4th of November 1995. From the very beginning the Canadian Ice Service (CIS) has been the prime user of the Radarsat SAR data for ice mapping (Ramsey et al., 1997). Both the experience from CIS and several EU projects (IMSI, OSIMS) and evaluation campaigns conducted by DMI have shown that Radarsat ScanSAR data is the most useful satellite data type for ice mapping. Radarsat is operating in a near circular polar orbit at an altitude of ~800 km, orbiting the earth ~14 times a day and has a 24 days repeat cycle. The C-band, horizontal linear polarised (HH) SAR is the only remote sensing instrument onboard the satellite and it can be operated in 14 different modes with varying resolution swath width etc. The ScanSAR wide mode is the mode most often used for ice mapping. DMI is receiving Radarsat SAR data both from Gatineau, in Canada, West Freugh in Scotland and Tromsø in Norway. Each of those tree processing facilities have different processors, data procedures and slightly different data formats, resulting in different data quality (ScanSAR data from West Freugh are not yet officially calibrated). The data used for wind extraction are all from Gatineau processing facility.

3. Site

Data treated in this report are from the Cape Farewell region (59-61°N,38-48°W). The Cape Farewell is the Southern point of Greenland. To the North East along the coast the East Greenland Current is transporting large quantities of Arctic sea ice into the area. The separation between the cold waters of the East Greenland Current and the warmer Atlantic waters in the Irminger Current, a branch of the Gulf Stream, is distinct often even detectable in Satellite imagery. The Julianehåb Bay (59.5°N-61°N,49°W-44°W) West of Cape Farewell is often sheltered from winds from the surrounding mountains, the bay is from February to August usually covered by sea ice. Weather conditions are severe in the Cape Farewell region where storms or fog are common (Gill et al. 1998).

4. Theory

4.1 Empirical theory of the interaction between electromagnetic radar waves and the ocean surface.

Scatterometry is measuring the wind near the sea surface using microwaves (Stoffelen, 1998). Scatterometry can be performed with scatterometers but in fact any active microwave instrument e.g. SAR.

The amplitude of the small scale capillary waves respond almost instantaneously to the local wind shear stress and align perpendicular to the local wind direction. The microwave scattering depend strongly on the amplitude of the capillary waves and the wave direction. The physical phenomenon that is important for the working of the scatterometer is the presence of capillary waves on the water surface. The ocean radar return is wind speed and direction dependent (Stoffelen, 1998).

The resonant scattering of the electromagnetic wave on the ocean surface is called Bragg scattering. Bragg scattering is dominating the microwave scattering from the ocean surface for moderate incidence angles. The condition for Bragg scattering is given by the relation:

wavelength_water = (n*wavelength_radar)/2*Sin(incidence_angle) (1)

The radar cross section (RCS) can then be approximated by:

RCS = T(incidence_angle)[E(2k)+E(-2k)] (2)

where k is the vector wave number of the radar beam with amplitude k=2phi/wavelength_radar, E is the spectral energy density of the short surface waves, and T is a transfer function describing the electromagnetic interaction with the ocean surface.

There is a relationship between the backscattered microwave power and the energy density of the gravity-capillary waves. There is also a relationship between the energy density of the gravity capillary waves and the wind shear stress over the ocean. Finally there is a relationship between the wind shear stress and the wind speed 10 m over the ocean surface.

The empirical relations between the normalised radar cross section (NRCS) the incidence angle and the wind speed and direction have been developed and validated for Scatterometer measurements. The ERS scatterometer for which the CMOD4 model was developed is operating in the vertical linear polarisation and was calibrated against measurements of wind speed and direction measured at buoys. For scatterometers which are measuring the same resolution cell from different look directions it is possible to derive both the wind speed and direction. However none of the space borne scatterometers in operation at the moment can derive the direction unambiguously. SAR data are only obtained from one look direction and it is therefore not possible to derive the wind speed without knowing the direction and deriving the direction without knowing the wind

speed. The wind direction can most often be found looking at the structure generated by the wind in the SAR image e. i. wind streaks.

4.1.1 Using SAR as scatterometer

Deriving wind speeds using SAR data has been demonstrated with success (Hortsmannet al. 2000 , Lehner et al. 1998 , Alpers and Brummer, 1994). The SAR winds can be obtained in very high resolution for example to resolve marine boundary layer (MBL) close to the coast (Horstmann et al. 1997) and boundary layer rolls (Alpers and Brummer, 1994) to find the optimal setting for wind turbines (Johannessen & Korsbakken, 1998) to study wind fields close to the ice edge (Tonboe et al. 1999), to study katabatic winds (Alpers et al. 1996) or the structure of hurricanes (Katsaros et al. 2000).

The ERS SAR is like the ERS scatterometer operating in the vertical linear polarisation and it therefore possible to adopt the wind algorithms developed for the ERS scatterometer to ERS SAR data. When the high resolution SAR data are used for the extraction of wind a number of issues must be addressed. For example speckle is apparent in all SAR data and for wind extraction it should be suppressed by appropriate averaging (discussed later). Also slicks, ocean waves, currents, sea ice etc. play a significant role in the SAR data which make the extraction of wind data from areas dominated by those physical artefacts impossible.

The approach taken to use Radarsat data for deriving wind speed has been to compensate the CMOD4 model, which was developed for vertical linear polarisation, to work also for the horizontal linear polarisation of Radarsat. The backscattered microwave power over open water is different than for the horizontal linear signal (Moore and Fung, 1979).
The empirical expression given by Thompson et al (1998) in formulae 3 can be used to prepare the HH polarised signal for the CMOD4 algorithmn.

$$NCRS(HH) = (1+\alpha \tan^2\theta)^2/(1+2 \tan^2\theta)^2 * NCRS(VV) \qquad (3)$$

α is 1 for the HH/VV compensation algorithm based on Kirchoff theory (Horstmann et al. 1999).

The determination of the empirical constant α is based on the collocated data set of 1) scatterometer measurements and ScanSAR wind measurements 2) HIRLAM model analysis and ScanSAR wind measurements (Horstmann et al., 2000).

4.1.2 SAR spectrum

The spectral energy density of (ERS) SAR data over the ocean surface varies with wave number. At high wave numbers the variation is dominated by speckle. At a spectral energy density of wave lengths in the order of ~300 m there is a local maximum in the energy density corresponding to the wavelength of ocean waves. From the ocean wave maximum of 300 m to a local energy density minimum at wavelengths of 2 km the influence of speckle decrease. At wavelengths of 2 km or greater the variation is dominated by variations in the wind stress (Horstmann et al. 2000). In this study all scenes have been spatially averaged to 2 * 2 km.

4.1.3 Application of the theory

Wind speeds can be extracted using SAR data whenever the conditions for scatterometry theory are met. The capillary waves at the sea surface must be in equilibrium with the local wind speed at 10 m above sea level and the surface must be affected by nothing but the wind. This practically means that wind speed can not be derived where there are surface slicks, where currents or density differences in the ocean is damping the capillary waves. The wind can naturally not be derived over sea ice or land. The uncertainty of the measurements is increased when the marine boundary layer is either stable or unstable or when the measurements are performed close to land or when the ocean surface is affected by rain. Also internal waves at the shelf and swells are affecting the microwave signal independently of the wind speed.

4.1.4 (Wind induced) features in SAR images

'The radar is a surface roughness sensor: the rougher the sea surface, the higher is the normalised radar cross section (NRCS)' (Brandt et al. 1996). The wind generated roughness is the major factor over the ocean but other mechanisms may play a role as well. Features on the ocean surface that may be seen in the SAR images of the Cape Farewell area are shortly described below using examples from the literature:

4.1.4.1 Atmospheric Gravity waves

Atmospheric gravity waves may be caused at the border between air masses of cold and warm air. Atmospheric gravity waves seen in SAR images have been studied by Thompson et al. (1992) off the Canadian Pacific coast. The marine atmospheric boundary layer where the gravity waves were propagating, was in this case stable but was capped by inversion. The waves were 1.3-2.3 kilometres long and were travelling in groups of about 10 waves. The group speed was about 6m/s parallel to the surface wind shear but with opposite propagation direction. The waves were generated at the border between an intruding unstable air mass and the stable air mass capped with the inversion.

4.1.4.2 Atmospheric Rolls

Rolls in the marine boundary layer are caused by instability in the lower atmosphere. The instability can be dynamic, in this case the rolling motion is generated by the changing wind velocity with height over the surface. The roll-axis is oriented perpendicular to a direction between the geostrophic wind direction and the surface wind direction. Often these rolls occur in an inversion capping situation, and the scale of the rolls are coincident with about half the depth of the marine boundary layer. If the instability is thermal (Rayleigh-Bernard instability) the wavelength of the rolls is 2-4 times larger than the height. The thermal rolling is caused either by cold air passing over a warm surface or by cold air over warm air. The roll axis is parallel to a wind direction between the surface wind direction and the geostrophic wind direction. Atmospheric boundary layer rolls contribute significantly to the vertical exchange of momentum, heat and moisture in the atmosphere. (Aplers and Brummer, 1994).

4.1.4.3 Ocean Tidal waves

Tidal wave trains have been studied by Brandt et al. (1996) in the Straight of Gibraltar: 'Internal waves become visible on radar images because they are associated with variable surface currents that modify the surface roughness patterns via current-wave interaction.' (Brandt et al., 1996). As the tidal currents flow through the Gibraltar Straight characteristic and predictable wave patterns are generated. The SAR is measuring the surface roughness of the ocean surface and the tidal waves are affecting the small scale surface waves. As a first order approximation the variation of the image intensity is proportional to the gradient of the sea surface velocity (Brandt et al., 1996).

Li et al. (2000) have studied ocean tidal waves in Radarsat SAR images at the shelf of the coast of New Jersey in order to determine the mixed layer depth. Their results were in fair agreement with salinity and temperature profile observations.

4.1.4.4 Wind fronts and cyclones

Cyclones and wind fronts can be seen in SAR images (Wu et al. 2000; Clemente-Colon and Yan, 2000) also wind shadowing can be studied in detail in coastal areas (Horstmann et al., 2000; Horstmann et al., 1997)

4.1.4.5 Stability of the atmosphere

At the border between cold and warmer waters, as for instance the border between the Gulf Steam and the colder North Atlantic waters, the stability of the air mass blowing across the border between the two water masses may change (Friedman and Li, 2000). When the wind is blowing from cold water across warmer waters the boundary layer becomes unstable and the wind speed apparently increases. This illustrate one of the problems deriving the wind speed at 10 m above the surface using SAR (or scatterometer) and not the wind shear on the surface. The wind estimate from Radarsat is not corrected for stability.

4.1.4.6 Storm cells

Storm cells seen in Radarsat SAR images are described by Friedman and Li (2000). The cell observed in the SAR image is rounded and one half is brighter than the other. This is a characteristic appearance during the downdraft stage of a rain/storm event. The air is dropping towards the centre of the cell and diverges as it reaches the ocean surface. The half of the cell where the diverging air is blowing against the general wind direction the wind speed is lower and the radar brightness is also lower, the half where the diverging air is blowing in the direction of the general wind the wind is enhanced and the radar brightness increased. Also differences in wind direction may be observed as differences in radar brightness in the SAR image of a Rain/storm cell.

During intense rain the capillary waves are damped by the impact of raindrops (Katsaros et al., 2000). An extreme result of intense rain may be observed by SAR. Atlas (1994) reports that intense rain on the ocean surface may create sufficient turbulence in the very ocean surface layer to damp the capillary surface waves and create echo-free 'holes' in the SAR image.

5. Data

5.1 Data transfer and form

The Radarsat data format is following the CDPF CEOS standard which is described in detail in CDPF CEOS SAR product format standard (1995). The data which are transferred to DMI are delivered in 5 separate files: Volume Directory File, SAR Leader File, SAR Data File, SAR Trailer, Null Volume Directory File. The actual data are contained in the SAR Data File and Important parameters which are used during the wind processing are contained in the SAR Trailer File and SAR Data File. The SAR data are represented by digital numbers (DN) as 8-bit unsigned integers. The data are received over the Internet. The data file is separated in 9-13 data blocks of approximately 10 Mbytes each during transfer. The trailer files are transferred as is. The transmission of the data has commenced minimum 4 hours from data acquisition. The data are also send to DMI on CD's these arrive in packages about 2 week after the image acquisition.

5.2 Data quality

During the SAR processing with the CDPF processor, a special ice look up table (ICE LUT) is used, developed for enhancing ice features. The calibration and development work on the processing facilities is resulting in continuously improving image quality. Latest when ScanSAR was declared officially calibrated in February 1999 making it possible to estimate the accuracy of the wind speeds derived from the data. However a visual inspection of the data will reveal several unwanted artefacts: 1) Scalloping is the periodic variation of DN in azimuth direction. The peak to peak distance for this variation in azimuth is about 1.2 km. Scalloping is caused by errors in Doppler parameter estimation, lately scalloping has been reduced considerably in the data received at DMI. 2) The Nadir ambiguity is a bright line in azimuth direction. It is found in all images where the satellite was situated over open water during the data acquisition. The Nadir ambiguity is due to a nadir reflection from the ocean surface, which is not compensated for during the processing. The satellite is over open water during data acquisition for all Cape Farewell images. 3) The ScanSAR principle combines raw data from different beam scans. For ScanSAR wide it is the beam combination w1,w2,w3 and s7. The data from the 4 different beam scans can be seen as 4 areas in range separated by small differences in DN between each area. This is caused by spacecraft attitude uncertainties (Beal, 2000). 4) Analogue to Digital Conversion (ADC) saturation is often a problem in the near range part of the image for open water. Even though Radarsat is operating with an automatic gain control, areas in near range sometimes reach saturation when the return power is distributed unevenly between the two half swaths, for example because of varying wind conditions. (Vachon et al. 1999, Vachon et al. 2000). 5) Range ambiguity is when echoes from one place are repeated in a different position in range. This is a very annoying artefact when the data are used for ice mapping.

The above mentioned artefacts reduce the absolute calibration accuracy of the SAR data. Radarsat estimates that the radiometric calibration accuracy at the moment (1999) is +/-1.35 dB (more for scallops). Beal (2000) mentions that as a result of spacecraft attitude alone an estimated wind speed of 25 m/s may be with up to 25% in error. The problem with the relative error on the wind speed is largest for high wind speeds and low incidence angles due to the form of the SAR wind algorithm (Horstmann et al. 2000).

6. Method

6.1 Data processing.

The wind speed can be derived from the Radarsat ScanSAR data if the incidence angle, normalised radar cross section (NRCS) and the wind direction is known. The DN can be transformed to NRCS using the knowledge of incidence angle and compensating the data for special enhancement procedures applied during the SAR processing.

The radar brightness is given according to the data compensation given by:

$$radar\_brightness[dB] = 10*\log_{10}[(DN^2 + offset)/lookup\_tab] \quad (4)$$

Offset, is a fixed offset related to the specific enhancement applied to the data during processing. In this case it is ICE processing, developed for enhancing ice features. Lookup_tab, is the special lookup table used during processing in this case to enhance ice.

The radar brightness is compensated for the incidence angle to give the NRCS:

$$NRCS[dB] = radar\_brightness + 10*\log_{10}(Sin(I)) \quad (5)$$

I, is the incidence angle.

To reduce speckle NRCS are averaged to 2*2 km pixels. The CMOD4 wind model is applied to the data considering the wind direction which can be estimated from wind streaks in the image. The wind speed algorithm is described in more detail in chapter 3.

After this the data follows a normal import scheme to the ERDAS/ArcView ice analysis system, including geocoding.

7. Results

First example of detailed Radarsat ScanSAR winds is a katabatic wind event south of Ammassalik on the Greenland East coast. The katabatic wind does not only continue over the sea ice drifting along the coast it also continues with almost unaltered strength 200 km over open water. The sea ice has been spread in the area with most wind.

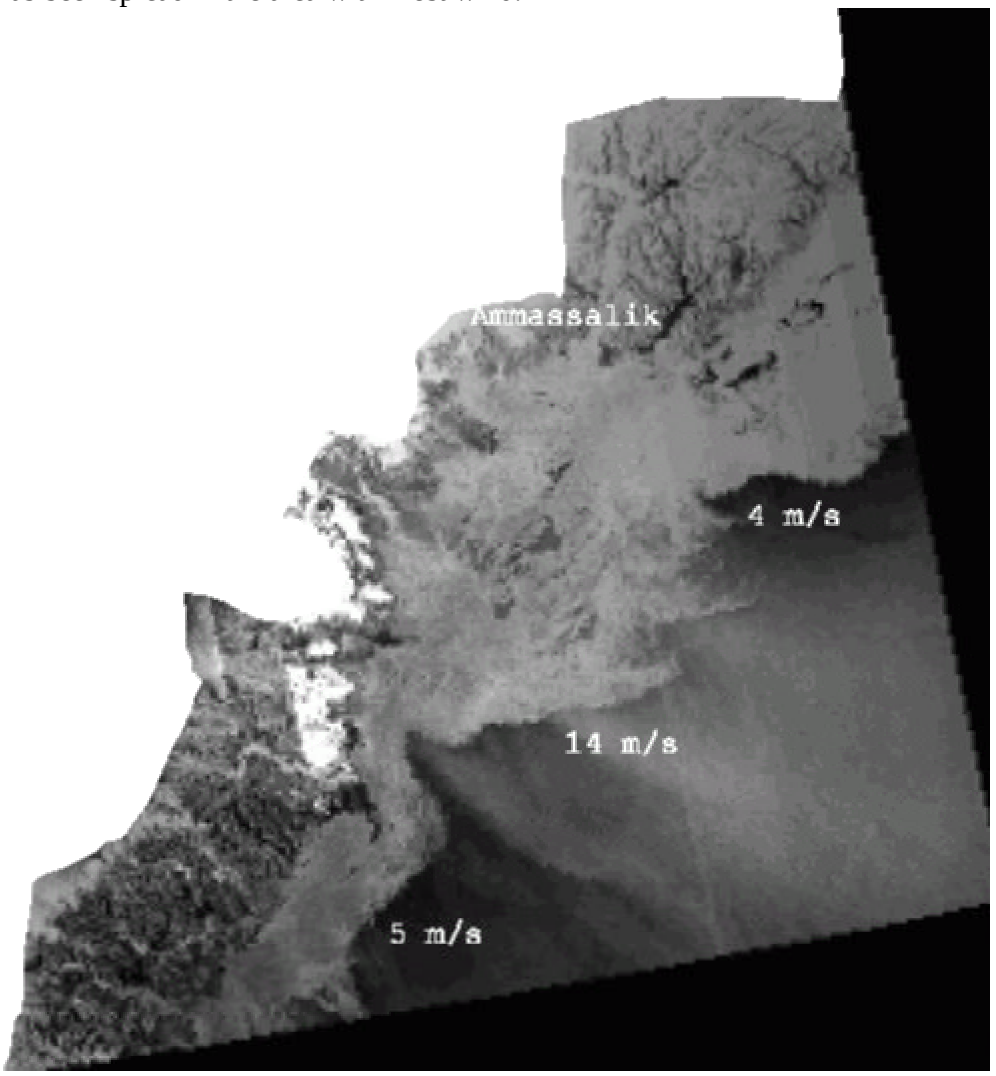

Figure 1. Katabatic wind off the coast of Ammassalik.

Second example is from the Cape Farewell in southern Greenland. The example illustrates the great variation of wind speeds which may be found in this area. These variations are not well resolved in neither model data nor scatterometer data.

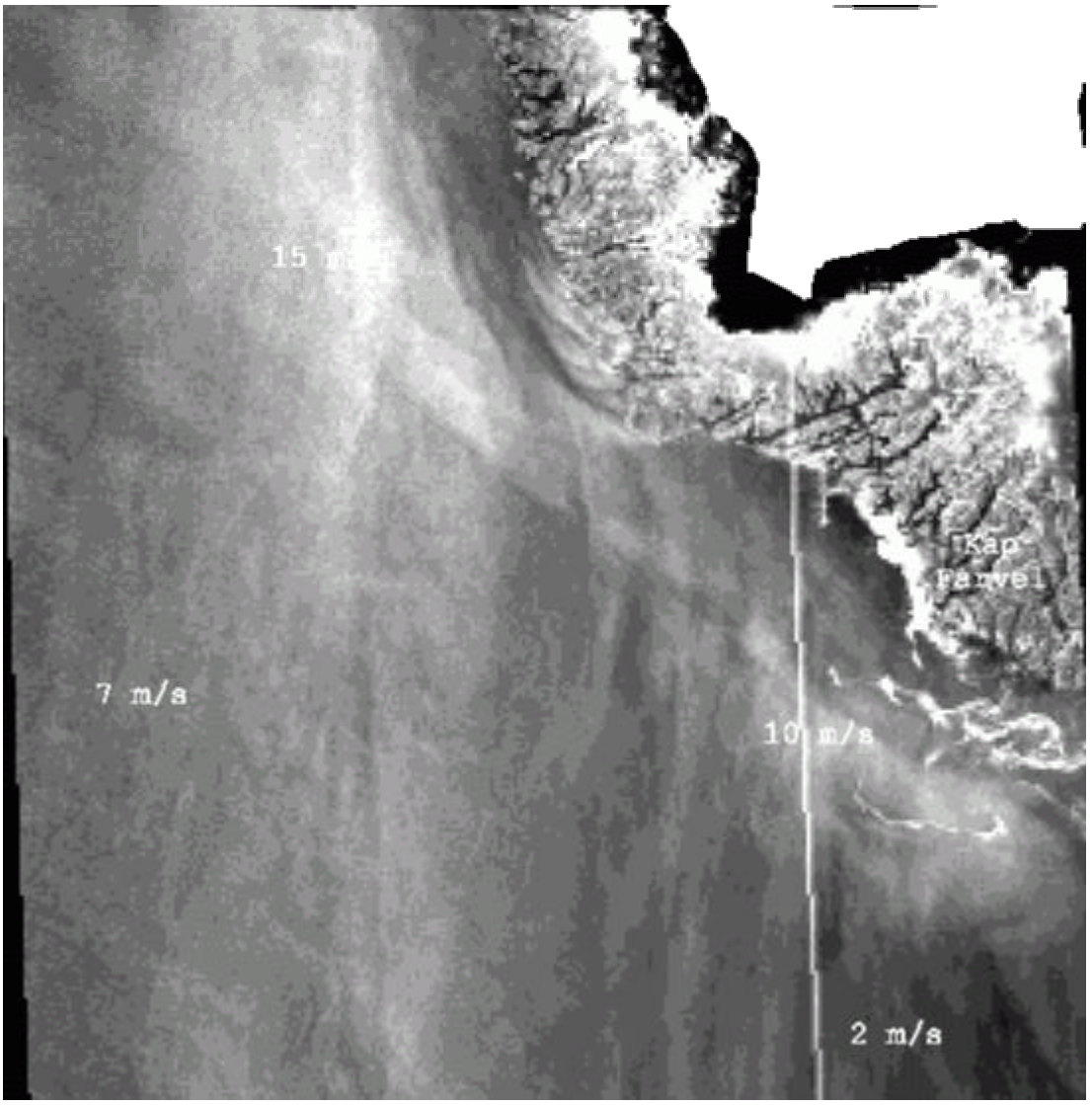

Figure2. Winds in the Cape Farewell Waters.

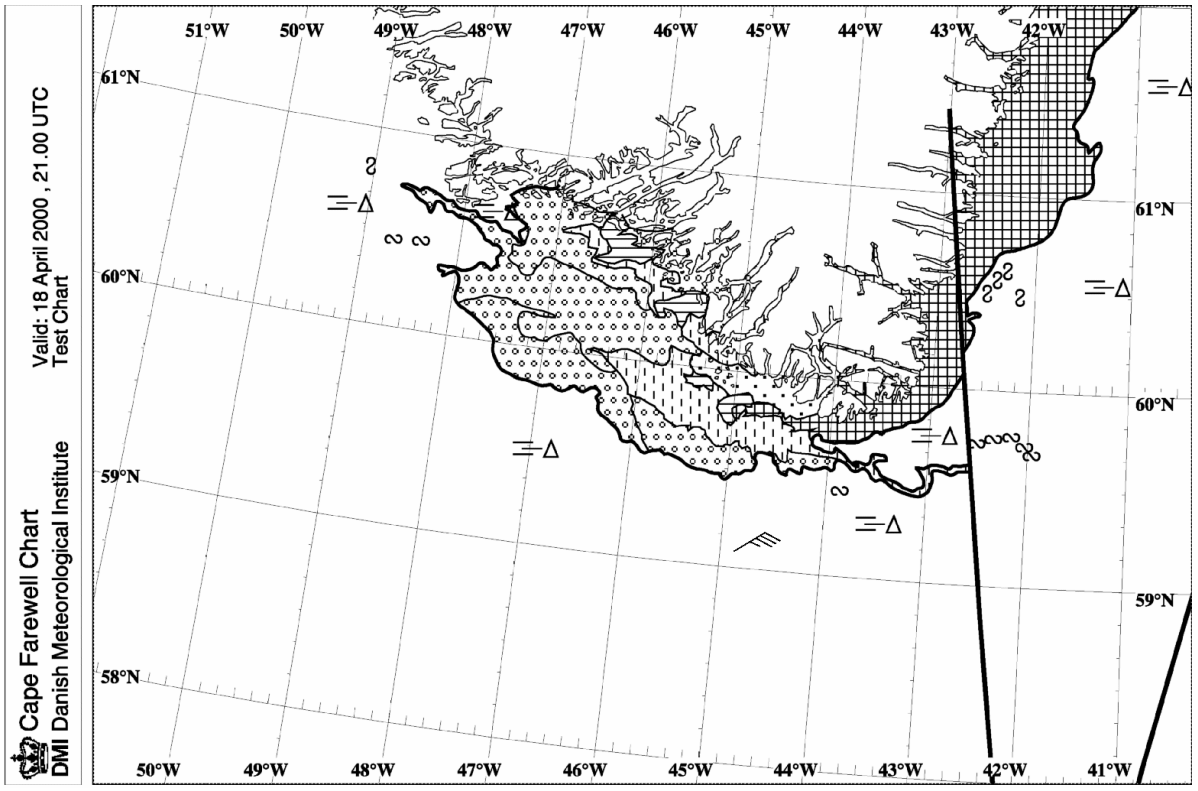

Figure 3. Cape Farewell ice chart 18th of April 2000 with wind vector from Radarsat.

8. Discussion and Conclusions

The local wind conditions in the Cape Farewell area are complex, but with great significance for the interpretation of SAR images and the sea ice drift. The sources for wind observations over the Cape Farewell waters are sparse. Some of the ships operating in the region is recording and reporting meteorological information to DMI. This information is very valuable and is always checked by the person in charge of the ice chart for the area. Also observations from the land stations is useful for the overview but an extrapolation of this information to the surrounding waters is difficult because of the effects from local topography on and around the station site.

The HIRLAM model is regularly producing both analysis and forecasts for the area. Even though the analysis is based on observations the model output is not validated over the Greenland waters and the accuracy of the model in this region cannot be determined.

The coverage of wind scatterometers have until recently been rather poor. The AMI SCAT onboard the ERS 1 and 2 satellites have been tested in the ice service. With the 500 km swath and the 24 day repeat cycle (the scatterometer is turned off when the SAR is operating) this instrument could not guarantee data whenever it was needed. For the local wind conditions the 25 km data resolution was too coarse. QuickScat was launched in June 1999 and it has a very attractive coverage with a 1800 km swath and daily 90% global coverage, however this data has not yet been tested in the ice service. The data resolution of QuickScat is like ERS 1 and 2 namely 25 km.

Deriving the wind speeds from the same data as are used for the operational ice mapping is attractive. The resolution of the measurements of 2 * 2 km is not matched by any other source, and makes it possible to detect even local wind conditions. The spatial variations in the wind field can be studied in detail.

The uncertainty of the measurements with Radarsat ScanSAR is not discouraging considering other data sources and the difficulties involved in doing measurements there.

One of the major drawbacks using Radarsat ScanSAR data for the wind measurements is that the measurements can only be done over open water. The wind speed over the sea ice is off course important when considering the ice drift. The wind speed over the ice must be extrapolated from the derived wind speeds over the sea.

For other applications of Radarsat winds than ice mapping the irregular temporal coverage represents a problem. Using the data during the ice analysis the temporal coverage is less important as the ice mapping is done with basis in the same data as are used for the Radarsat winds. During stable weather conditions the details of the situation may be read from the data interpreting the wind and the ice situation at the same time.

9. References

Alpers, W., and B. Brummer (1994): *Atmospheric boundary layer rolls observed by the synthetic aperture radar aboard the ERS-1 satellite.* Journal of Geophysical Research. Vol. 99, No.: C6, pp. 12613-12621.

Alpers, W., U. Pahl, G. Gross, and D. Etling (1996): *Study of katabatic wind fields by using ERS-1 synthetic aperture radar imagery of the ocean surface*. Presented at IGARSS 1996.

Atlas, D. (1994*): Footprints of storms on the sea: A view from spaceborne synthetic aperture radar*. Journal of geophysical research, Vol. 99, No. C4, pp. 7961-7969.

Brandt, P., W. Alpers, and J. O. Backhaus (1996): *Study of the generation and propagation of internal waves in the Straight of Gibraltar using a numerical model and synthetic aperture radar images of the European ERS 1 satellite.* Journal of geophysical research, Vol. 101, No. C6, pp. 14237-14252.

CDPF CEOS SAR data products format standard. Ref: RZ-SP-50-5313, Issue/Revision: 5/0, Date: JUL. 11, 1995.

Clemente-Colon, P. and X. H. Yan (2000): *Low Backscatter Ocean Features in Synthetic Aperture Radar Imagery*. John Hopkins APL, Technical Digest, Coastal and Marine Applications of Wide Swath SAR, January-March 2000, Volume 21, Number 1.

Friedman, K. S., and X. Li (2000*): Monitoring hurricanes over the ocean with wide swath SAR.* John Hopkins APL, Technical Digest, Coastal and Marine Applications of Wide Swath SAR, January-March 2000, Volume 21, Number 1.

Gill, R. S., and H. H. Valeur (1999): *Ice cover discrimination in the Greenland waters using first order texture parameters of ERS SAR images*. Int. Journal of Remote Sensing, Vol. 20, No. 2, pp. 373-385.

Horstmann, J., W. Koch, S. Lehner, E. Romaneessen, R. Tonboe (2000): *Extraction of Ocean wind fields using Radarsat-1 ScanSAR images*. Presented at the Sixth International Conference on Remote Sensing for Marine and Coastal Environments, Charleston, South Carolina, 1-3 May 2000.

Horstmann, J., W. Koch, W. Rosenthal and S. Lehner (1997): *Wind fields from ERS SAR, compared with a mesoscale atmospheric model near to the coast*. Proc. Of the third ERS Symposium, Space at the service of our Environment, Florence, Italy 17-21 March 1997.

Johannesen, O. M., and E. Korsbakken (1998): *Determination of wind energy from SAR images for citing windmill locations*. Earth observation Quarterly, ESA, EOQ No.:59, June 1998.

Katsaros, K. B., P. W. Vachon, P. G. Black, P. P. Dodge, and E. W. Uhlhorn (2000*): Wind Fields from SAR: Could They Improve Our Understanding of Storm Dynamics*? John Hopkins APL, Technical Digest, Coastal and Marine Applications of Wide Swath SAR, January-March 2000, Volume 21, Number 1.

Moore, R. K., and A. K. Fung (1979): *Radar Determination of Winds at Sea*. Proceedings of the IEEE, Vol. 67, No. 11, November 1979.

Ramsey, B., L. Weir, K. Wilson and D. Bradley (1997): *Utilisation of Radarsat Data in the Canadian Ice Services. Geomatics in the era of Radarsat*, GER'97 symposium, Ottawa, May 25th-30th.

Shepherd, N. (1998): *Extraction of Beta Nought and Sigma Nought from RADARSAT CDPF products*, Report No.: ALTRIX Systems 97-5001, Prepared for: S. Srivastava, CSA, Contract No.: 9F005-6-0025/001/SN.
Stoffelen, A. (1998): *Scatterometry*. PhD Thesis. CIP gegevens Koninklijke Bibliotheek, Den Haag.
Thompson, R. E., P. W. Vachon, G. A. Borstad (1992): *Airborne Synthetic Aperture Radar Imagery of Atmospheric Gravity Waves*. Journal of geophysical research, Vol. 97, No. C9, pp. 14249-14257.
Tonboe, R. T., R. S. Gill and J. Horstmann (1999): *Near ice edge estimation of the sea surface winds using Radarsat ScanSAR.* Presented at EUMETSAT Meteorological Satellite Data Users' Conference, Copenhagen, Denmark, 6th - 10th September 1999.
Wu, S., A. Liu, G. Leonard and W. G Pichel (2000): *Ocean feature monitoring with wide swathe synthetic aperture radar*. John Hopkins APL, Technical Digest, Coastal and Marine Applications of Wide Swath SAR, January-March 2000, Volume 21, Number 1.

9.1 Project publications

Horstmann, J., W. Koch, I. Weinreich, S. Lehner, and R. Tonboe, *Computation of Ocean Wind Vectors Using RADARSAT ScanSAR and ERS SAR images*, in Proceedings of IEEE 1999 International Geoscience and Remote Sensing Symposium, Hamburg, Germany, Vol.III, pp. 1625-1627, 1999.
Horstmann, J., S. Lehner, W. Koch, and R. Tonboe, *Computation of Wind Vectors over the Oean Using Sapceborne Synthetic Aperture Radar*, Johns Hopkins APL Technical Digest, Vol. 21, Nr.1, pp. 100-107, 2000.
Horstmann, J., S. Lehner, W. Koch, J. Schulz-Stellenfleth, and R. Tonboe, *Wind Retrieval over the Ocean Surface using Synthetic Aperture Radars*, in Proceedings of CEOS SAR Workshop, Toulouse, France, in press 2000.
Horstmann, J., W. Koch, S. Lehner, E. Romaneessen, and R. Tonboe, *Extraction of Ocean Wind Fields Using RADARSAT-1 ScanSAR Images*, in Proceedings of the Sixth International Conference on Remote Sensing for Marine and Coastal Environments, Charleston, South Carolina, 1-3 May, in press 2000.
Horstmann, J., W. Koch, S. Lehner, and R. Tonboe, *Wind Retrieval over the Ocean using Synthetic Aperture Radar with C-band HH Polarization*, IEEE Transaction on Geoscience and Remote Sensing, accepted 2000.
Horstmann, J., W. Koch, S. Lehner, and R. Tonboe, *Wind Speed Retrieval From RADARSAT-1 ScanSAR, in Proceedings of EuSAR 2000 3rd European Conference on Synthetic Aperture Radars*, Munich, Germany, 23-25 May, submitted 2000.
Tonboe, R.T., R.S. Gill, and J. Horstmann, *Near Ice Edge Estimation of the Surface Winds Using RADARSAT ScanSAR*, in Proceedings of the 1999 EUMETSAT Meteorological Satellite Data Users Conference, Copenhagen, Denmark, in press 2000.